Canadian Mineralogist
Vol. 28, pp. 93-109 (1990)

EVALUATION OF THE RIETVELD METHOD FOR THE CHARACTERIZATION OF FINE-GRAINED PRODUCTS OF MINERAL SYNTHESIS: THE DIOPSIDE–HEDENBERGITE JOIN

MATI RAUDSEPP, FRANK C. HAWTHORNE AND ALLAN C. TURNOCK

Department of Geological Sciences, University of Manitoba, Winnipeg, Manitoba R3T 2N2

ABSTRACT

We have evaluated the Rietveld method for characterizing fine-grained products of mineral synthesis by refining the crystal structures of a series of synthetic clinopyroxenes along the diopside – hedenbergite join. The Rietveld method uses the whole powder-diffraction pattern to characterize the structure of a material; the structural parameters (atomic positions, site occupancies, displacement parameters), together with various instrumental parameters, are refined by least-squares procedures to minimize the difference between the complete observed and calculated diffraction-patterns. With this technique, more than one phase can be refined simultaneously. Step-scan X-ray powder diffraction data were collected over the range 17–130°2θ using Cu$K\alpha$ X radiation. The structures of the synthetic clinopyroxenes were refined to R_B indices of 1.8–3.5% and R_{wp} indices of 8.0–11.4%. For diopside, comparison with single-crystal results on natural material shows good agreement between the structural parameters, but half-normal probability analysis shows the Rietveld standard deviations to be underestimated by a factor of ~1.6; this was expected, as the Durbin–Watson *d*-statistic (1.39) indicates the presence of significant serial correlation. For the Fe-bearing pyroxenes, the observed stereochemistry agrees with that expected for pyroxenes intermediate between the known structures of diopside and hedenbergite. Unconstrained site-occupancy refinement (with isotropic displacement factors fixed at appropriate single-crystal values) indicates $M(2)$ = Ca; the refined $M(1)$ occupancies are within 2 standard deviations (σ = 0.01 a.p.f.u.) of the nominal compositions, but are systematically lower, suggesting that the synthesized pyroxenes may be slightly off-composition. For the two-phase products, the (fixed) structure of ferrobustamite was incorporated into the refinement procedure, and the site occupancies, cell dimensions and scale factor (a measure of modal amount) were refined concurrently with the accompanying pyroxene. Model calculations show that the minimum in the site-occupancy refinement is well-defined, provided that the displacement factors are fixed (at appropriate values). Site occupancies are dependent on the values of the displacement factors used, but model calculations show that a fairly large range in B (± 0.25Å^2) spans only 1 standard deviation (0.01 a.p.f.u.) of a Mg–Fe site occupancy. Thus site-occupancy refinement is not impractically dependent on the displacement factors used. Unconstrained site-occupancy refinement gives us not only the site occupancies, but also the bulk compositions of the pyroxene; the close agreement between the nominal and refined compositions indicates that this may be a viable technique for compositional determination of *suitable* fine-grained minerals. In addition, multiphase mixtures may be analyzed, with the possibility of determining cation occupancies, bulk compositions and modal proportions for each phase. These factors indicate that Rietveld structure refinement will be of major importance in characterization of products of synthesis in the future.

Keywords: Rietveld method, diopside, hedenbergite, structure refinement, fine-grained materials, multiphase assemblages, products of syntheses.

SOMMAIRE

Nous avons évalué la méthode de Rietveld pour caractériser les produits de synthèse à grains fins par l'affinement de la structure cristalline de clinopyroxènes de la série diopside – hédenbergite. Cette méthode utilise le cliché de diffraction au complet pour calculer la structure du matériau. Les paramètres structuraux (positions atomiques, répartition parmi les sites, paramètres de déplacement), ainsi que les divers paramètres instrumentaux, ont été affinés par moindres carrés afin de minimiser la différence entre le cliché de diffraction observé et calculé. Il est même possible de caractériser plus d'une phase à la fois. La lecture des intensités diffractométriques s'est faite selon le mode "step-scan" entre 17 et 130° 2θ (rayonnement Cu$K\alpha$). Les structures ont été affinées jusqu'à un résidu R_B entre 1.8 et 3.5%, et une valeur de R_{wp} entre 8.0 et 11.4%. Pour le diopside, les résultats obtenus sur cristal unique naturel montrent une bonne concordance des paramètres structuraux, mais une analyse de probabilité demi-normale démontre que les écarts-types pour la méthode de Rietveld seraient sous-estimés par un facteur d'environ 1.6; c'est une déviation anticipée, puisque la statistique d de Durbin–Watson (1.39) indique la présence d'une corrélation sérielle importante. Pour les compositions riches en fer, la stéréochimie observée concorde avec les résultats anticipés pour les compositions intermédiaires entre les pôles diopside et hédenbergite. Les affinements d'occupation de sites sans contraintes (avec des facteurs de déplacement isotrope fixés selon les résultats obtenus sur cristaux uniques correspondants) indiquent que $M(2)$ contient le Ca; $M(1)$ contient, à deux écarts-type près (σ = 0.01 atomes par unité formulaire), les populations prévues selon les compositions préparées, mais les occupations sont systématiquement incomplètes, ce qui fait penser que la composition des produits synthétiques est légèrement non stoechiométrique. Pour les produits à deux phases, la structure (fixée) de la ferrobustamite a été incorporée dans la procédure d'affinement, et les occupations des sites, les paramètres réticulaires, et le facteur d'ajustement (mesure de la proportion des volumes) ont été affinés simultanément avec ceux du pyroxène pré-

sent. Le minimum dans la fonction d'occupation des sites serait bien défini, d'après nos calculs, pourvu que les facteurs de déplacement soient fixés (à des valeurs appropriées). Les occupations des sites dépendent des valeurs choisies pour ces facteurs, mais des calculs modèles montrent qu'un intervalle assez grand de valeurs de B ($\pm$ 0.25Å^2) correspond à seulement un écart-type (0.01 atomes par unité formulaire) dans l'occupation du site (Mg,Fe). C'est donc dire que l'affinement de l'occupation d'un site ne dépend pas de façon non pratique des facteurs de déplacement choisis. L'affinement sans contraintes de l'occupation des sites mène en plus à la composition globale d'un pyroxène; la concordance étroite entre la composition prédite et affinée montre que cette technique pourrait bien servir pour déterminer la composition de matériaux à grain fin appropriés. De plus, la possibilité existe d'analyser des assemblages multi-phasés et de déterminer la répartition des cations, la composition globale et la proportion modale de chaque phase. Pour ces raisons, il paraît évident que l'affinement des structures par la méthode de Rietveld aura une grande importance dans la caractérisation des produits de synthèse.

(Traduit par la Rédaction)

Mots-clés: méthode de Rietveld, diopside, hédenbergite, affinement de la structure, matériaux à grains fins, assemblages multi-phasés, produits de synthèse.

TABLE 1. NOMINAL COMPOSITIONS, CONDITIONS AND PRODUCTS

Run No.	Composition	T (°C)	Products
D0	$CaMgSi_2O_6$	1330	cpx + (crs)
D2	$CaMg_{0.8}Fe_{0.2}Si_2O_6$	1288	cpx + glass
D3	$CaMg_{0.7}Fe_{0.3}Si_2O_6$	1222	cpx + (fbs)
D5	$CaMg_{0.5}Fe_{0.5}Si_2O_6$	1150	cpx + (fbs)
D7	$CaMg_{0.3}Fe_{0.7}Si_2O_6$	1120	cpx + fbs + (crs) + (ol)

cpx: clinopyroxene; fbs: ferrobustamite; crs: cristobalite; ol: olivine.

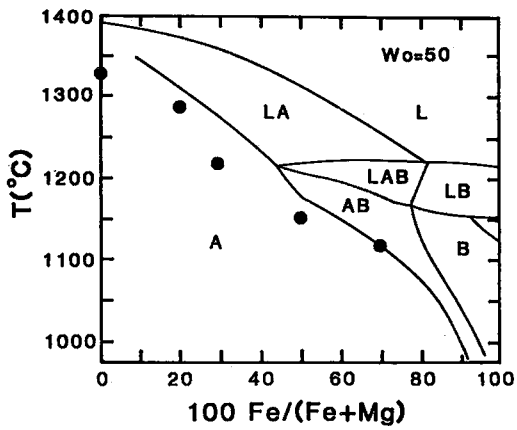

FIG. 1. Temperature-composition section along the diopside-hedenbergite join at 1 atm and low oxygen fugacity, showing T, X and phases of refined products (after Huebner & Turnock 1980). Symbols: A augite; B pyroxenoid, ferrobustamite; L liquid.

INTRODUCTION

A significant problem in studies of mineral synthesis and stability is the characterization of the run products. These are commonly quite fine-grained (of the order of a few micrometers), and consequently are difficult to characterize adequately. The techniques traditionally used are optical microscopy and X-ray powder diffraction; however, these can rarely provide quantitative information on phase composition and intracrystalline order. Although small particles can be analyzed by electron microprobe (*e.g.*, White 1964, Spear 1981), this approach provides no information on the degree of order of the constituent phase(s). Spectroscopic techniques are now being used more frequently for this purpose (Hawthorne 1988), but tend to be too problem-specific to constitute a general-purpose method. We have advocated the use of the Rietveld method for better run-product characterization (Raudsepp *et al.* 1982, 1984, Hawthorne *et al.* 1984). The method (Rietveld 1967, 1969) uses the whole powder-diffraction pattern to characterize the *structure* of a material; the structure parameters of the mineral [atomic coordinates, site occupancies and displacement (thermal) parameters], together with various experimental parameters affecting the pattern, are refined by least-squares procedures to minimize the difference between the complete observed and calculated diffraction-patterns. Although the Rietveld method was used originally for the refinement of fairly simple structures with X-ray-diffraction data (Young *et al.* 1977, Khattak & Cox 1977, Young 1980), it has since proved quite powerful for complicated structures (Baerlocher 1984, Baerlocher & Schicker 1987, Ercit *et al.* 1985, Raudsepp *et al.* 1987a, b). In addition, it is also possible to refine the structures of more than one phase simultaneously, and thus the method is applicable to *assemblages* of synthesized minerals; indeed, the modal amounts of each phase also can be derived by this method. Additional advantages are: (i) the equipment used, an X-ray powder diffractometer, is widely available; (ii) there is extensive readily available software for structure refinement (Hill & Howard 1986, Larson & von Dreele 1988, Wiles & Young 1981, Baerlocher 1982).

We have long been interested in the synthesis, characterization and phase relations of Ca–Mg–Fe pyroxenes (Turnock 1962, 1970, Turnock *et al.* 1973). In these previous studies, the synthesized pyroxenes were assumed to be of nominal composition, and the degree of order over the $M(1)$ and $M(2)$ sites was not characterized. For single-phase material, examination by Rietveld structure refinement can provide information on degree of order, and information on stereochemistry (although this cannot be as good in quality as analogous single-crystal data). For multiphase material, Rietveld struc-

ture refinement can provide compositions, information on the degree of order of all phases, and their modal proportions. This being the case, it will greatly increase the information derived from synthesis and phase-equilibrium studies, and provide much more complete information for thermodynamic modeling.

In the past 30 years, many new techniques of characterization have been introduced into mineralogy. These have usually followed the same cycle of development. They have been introduced to mineralogy with strong (usually exaggerated) claims of accuracy, but with no adequate study of either precision or accuracy. This has eventually led to the (undeserved) discreditation of the method, and it has taken a further 10 years or so to re-establish it as a standard credible method of characterization. The principal thrust of the current work is to establish the utility of the method and to demonstrate the precision and accuracy that can be expected for geologically useful minerals; hopefully we can bypass the discreditation phase of the cycle outlined above. In order to provide a realistic evaluation of accuracy, we examine here a simple but geologically relevant system: single- and multi-phase products of synthesis along the diopside – hedenbergite join, from diopside ($Wo_{50}En_{50}Fs_0$) to hedenbergite ($Wo_{50}En_{15}Fs_{35}$). Nominal compositions are given in Table 1, together with conditions of synthesis and nature of the products; phase relations are shown in Figure 1. The crystal structures of diopside (Clark *et al.* 1969, Levien & Prewitt 1981) and hedenbergite (Cameron *et al.* 1973) are well known, and provide good constraints on the possible stereochemical variations to be expected in our intermediate binary compositions. In addition, the bulk-composition constraints imposed by the simple nominal chemistry provide a good check on the accuracy of the refined bulk-compositions. If the refined structures are reasonable, we can expect good results for the chemically more complex ternary pyroxenes.

Experimental Methods

Synthesis

Clinopyroxenes were synthesized from mixtures of dry reagent-grade $CaCO_3$, Fe_2O_3, SiO_2 and MgO by repeated heating and grinding cycles (Turnock *et al.* 1973). Sample pellets were suspended from Pt wire hangers and heated at temperatures 10 to 60°C below the solidus in the range 1120 to 1330°C at 1 atm pressure. Oxygen fugacity was maintained near the iron–wüstite buffer by passing a gas mixture ($CO/CO_2 = 3$) through the furnace. After each experiment, the product was ground for 15 minutes under xylol in an alundum or agate mortar. After 10 cycles, the Mg-rich run products were found to contain mainly prismatic clinopyroxene crystals up to 30 μm in length, with rare (< 0.5%) olivine and cristobalite; Fe-rich products also contain up to about 8% ferrobustamite. Nominal compositions, conditions of synthesis, and products are listed in Table 1 and are shown graphically in Figure 1.

Data collection

Samples were mounted in standard aluminum sample holders with 20 x 15 x 1.6 mm cavities. Thus with a 1° divergence slit, the irradiated area was confined to the sample at 2θ angles greater than 19°. Two different methods of mounting were used. For cell-dimension determination, powders were densely packed from the back of the mount against a frosted glass slide; this procedure gave a flat surface level with the top of the holder, a surface that was consistent from sample to sample; thus specimen-displacement and transparency errors are minimized (Wilson 1963). Intensity data collected in this fashion are unsuitable for structure refinement because the resultant tight packing against a flat surface greatly exaggerates preferred orientation. Mounts for intensity-profile data were made by loading the powder from the front of the sample holder, leveling the surface flush with the mount with a straight-edge, and finely serrating the surface of the sample with a razor blade several times; each pass with the razor blade was at right angles to the previous one. This technique tends to randomize the orientation of anisotropic crystals that are aligned during filling, but maintains a generally flat surface.

TABLE 2. DATA COLLECTION AND DETAILS OF STRUCTURE REFINEMENT

	D0	D2	D3	D5	D7
2θ scan range (°)	17–130	17–130	17–130	17–70	17–70
Step interval (°2θ)	0.12	0.12	0.12	0.12	0.12
Integration time/step (s)	2	2	2	2	2
Maximum step intensity (counts)	3185	4598	3929	2371	2610
No. of phases refined	1	1	1	2	2
No. of unique reflections (cpx)	394	393	396	99	99
No. of unique reflections (fbs)	–	–	–	313	310
No. of structure parameters (cpx)	19	19	19	19	19
No. of structure parameters (fbs)	–	–	–	10	10
No. of experimental parameters (cpx)	13	13	12	13	13
No. of experimental parameters (fbs)	–	–	–	1	1
Scale factor (cpx) $\times 10^3$	0.890	0.688	0.701	0.513	0.346
Scale factor (fbs) $\times 10^3$	–	–	–	0.012	0.032
$N - P$	911	911	912	399	400
R_p	7.2	7.5	8.4	5.9	6.1
R_{wp}	9.7	10.4	11.4	8.0	8.8
R_B (cpx)	3.27	3.15	3.52	1.78	2.49
R_B (fbs)	–	–	–	3.13	3.57
Durbin-Watson d-statistic	1.39	1.63	1.56	1.77	1.62
U (cpx)	0.049	0.048	0.069	0.409	0.291
V (cpx)	–0.020	0.043	0.040	–0.211	–0.134
W (cpx)	0.104	0.030	0.030	0.086	0.080
γ_1 (cpx)	0.355	0.372	0.542	0.664	0.402
γ_2 (cpx)	0.006	0.001	0.006	0.005	0.002

cpx: clinopyroxene; fbs: ferrobustamite

$N - P$: no. of observations (steps) – no. of least-squares parameters.

Step-scan powder-diffraction data were collected with a Philips automated diffractometer system PW1710, using a PW1050 Bragg–Brentano goniometer equipped with incident- and diffracted-beam Soller slits, 1° divergence and anti-scatter slits, a 0.2-mm receiving slit and a curved graphite diffracted-beam monochromator. The normal-focus Cu X-ray tube was operated at 40 kV and 40 mA, using a take-off angle of 6°. The profiles were taken using a step interval of $0.12°2\theta$, with a step counting time of 2 s. As discussed by Hill & Madsen (1986), these are approximately the optimum parameters for reducing serial correlation without adversely affecting the accuracy of these results. Information pertinent to data collection is given in Table 2.

Rietveld structure refinement

Structures were refined with the Rietveld program *LHPM1* (Hill & Howard 1986). The peaks were defined as pseudo-Voigts with percentage Lorentzian character varied according to the function

$$\gamma = \gamma_1 + \gamma_2 2\theta, \quad (1)$$

where γ_1 and γ_2 are refinable parameters. The variation of the peak full-width at half-maximum (FWHM) was defined by the function of Caglioti *et al.* (1958)

$$H_k = (U\tan^2\theta + V\tan\theta + W)^{0.5}, \quad (2)$$

where U, V and W are refinable parameters. Backgrounds were fitted with a simple polynomial function. The profile-step intensity was calculated over the interval of four FWHM on either side of each peak centroid; peak asymmetry was corrected as a function of 2θ. Initial structural parameters were taken from the single-crystal study of diopside (Levien & Prewitt 1981); isotropic displacement factors were fixed at the single-crystal values. Information pertinent to the structure refinements is given in Table 2.

TABLE 3. CELL DIMENSIONS OF CLINOPYROXENE AND FERROBUSTAMITE

	a (Å)	b (Å)	c (Å)	α (°)	β (°)	γ (°)	V (Å³)
			Pyroxene				
Di[1]	9.7456(7)	8.9198(8)	5.2516(5)		105.86(1)		439.13(6)
D0	9.7470(7)	8.9235(4)	5.2524(4)		105.939(4)		439.28
D2	9.7634(8)	8.9488(7)	5.2504(4)		105.726(4)		441.56
D3	9.7730(7)	8.9523(6)	5.2524(3)		105.676(4)		442.44
D5	9.795(1)	8.979(1)	5.2545(7)		105.500(8)		445.34
D7	9.814(1)	8.9959(9)	5.2534(6)		105.331(8)		447.29
			Ferrobustamite				
fbs[2]	7.691	7.112	13.765	90.37	95.27	103.97	727.2
D5	7.733(7)	7.143(5)	13.790(9)	90.2(2)	95.2(1)	103.72(8)	736.69
D7	7.702(3)	7.119(2)	13.789(4)	90.48(5)	95.16(4)	103.83(2)	730.82

[1]diopside (Levien & Prewitt 1981)

[2]ferrobustamite, $Wo_{50}Fs_{50}$ (Rapoport & Burnham 1973)

After estimating as closely as possible the initial structural and experimental parameters both from the single-crystal structure and by inspection of the pattern, refinements were done in the following sequence. First, the scale factor, zero-point correction and background parameters were refined with all other parameters fixed, followed by the cell dimensions. Next, the half-width parameters were added in the order W, U, V; these are the most difficult parameters to refine, and occasionally some manual adjustment was necessary in order to achieve convergence. The remaining parameters were added to the refinement in the order: peak shape (γ_1), peak asymmetry, atomic positions, site occupancies, peak shape (γ_2) and correction for preferred orientation. In the refinements of two-phase products, only the scale factor, cell dimensions and octahedral site occupancies of ferrobustamite were refined; peak parameters were fixed to be those of pyroxene, and structural parameters were fixed at those from the single-crystal refinement of $Ca_{0.5}Fe_{0.5}SiO_3$ (Rapoport & Burnham 1973). These constraints were necessary because the low symmetry of ferrobustamite (large number of reflections) results in a large number of variable parameters, coupled with a decrease in the information content of the pattern due to increased peak-overlap with the major pyroxene phase. Final convergence of the refinements was assumed when the parameter shifts in the final cycle were less than 30% of their respective standard deviations.

Experimental Results

Single-phase structure refinement

The Rietveld method uses the *whole* powder-diffraction pattern (point by point) to characterize the structure of the material examined; the difference between the calculated and observed patterns is minimized by least-squares procedures. Such step-scan data are prone to serial correlation of the least-squares residuals, and incorrect estimates of parameter variances (precision) are inevitable if the step widths and counting times at each step are not optimized. Thorough studies by Hill & Flack (1987) and Hill & Madsen (1984, 1986) have shown that serial correlation is significantly influenced by the choice of step widths and counting times at each step; however, the *accuracy* of the structural parameters is *not* significantly affected (within sensible limits). They also showed that the Durbin-Watson d-statistic (Durbin & Watson 1950, 1951, 1971) is a sensitive measure of the presence of such serial correlation, and it should routinely be used as a means of assessing the reliability of the derived standard deviation of a parameter. We obtained d-statistics between 1.39 and 1.77 for the pyroxene refinements,

TABLE 4. ATOMIC POSITIONS FOR CLINOPYROXENE

		Di[1]	D0	D2	D3	D5	D7
M(1)	x	0	0	0	0	0	0
	y	0.90814(5)	0.9071(8)	0.9090(6)	0.9080(7)	0.9078(8)	0.9056(8)
	z	0.25	0.25	0.25	0.25	0.25	0.25
	B (Å^2)	0.37(1)					
M(2)	x	0	0	0	0	0	0
	y	0.30144(3)	0.2995(5)	0.2999(5)	0.3000(6)	0.2973(9)	0.2972(10)
	z	0.25	0.25	0.25	0.25	0.25	0.25
	B (Å^2)	0.635(8)					
T	x	0.28627(3)	0.2857(5)	0.2875(4)	0.2873(5)	0.2894(8)	0.2879(8)
	y	0.09330(3)	0.0943(5)	0.0928(5)	0.0932(6)	0.0922(9)	0.0920(10)
	z	0.22936(5)	0.2312(8)	0.2323(8)	0.2323(9)	0.2321(15)	0.2310(16)
	B (Å^2)	0.349(8)					
O(1)	x	0.11550(7)	0.1144(9)	0.1162(8)	0.1169(9)	0.1182(13)	0.1192(14)
	y	0.08728(7)	0.0900(11)	0.0896(10)	0.0912(11)	0.0897(17)	0.0909(20)
	z	0.1422(1)	0.1420(16)	0.1403(16)	0.1453(17)	0.1508(28)	0.1458(28)
	B (Å^2)	0.51(1)					
O(2)	x	0.36136(7)	0.3619(10)	0.3610(9)	0.3623(9)	0.3644(12)	0.3607(14)
	y	0.25013(8)	0.2516(9)	0.2488(8)	0.2488(9)	0.2480(14)	0.2498(16)
	z	0.3183(1)	0.3176(17)	0.3184(16)	0.3227(18)	0.3233(28)	0.3210(30)
	B (Å^2)	0.65(1)					
O(3)	x	0.35083(7)	0.3499(11)	0.3520(10)	0.3505(11)	0.3514(16)	0.3525(17)
	y	0.01759(8)	0.0185(9)	0.0175(9)	0.0178(10)	0.0160(15)	0.0188(16)
	z	0.9953(1)	0.9974(21)	0.9968(20)	0.9980(22)	0.9970(36)	0.9916(38)
	B (Å^2)	0.56(1)					

[1]diopside, single-crystal structure (Levien & Prewitt 1981)

consistent with moderate positive serial correlation.

At the outset of this study, we tried refinements with step widths of 0.08 to 0.24°2θ and counting times of 2 to 5 s at each step. Our results confirmed those of the previous studies. However, step widths wide enough to avoid serial correlation (~ 80% of the minimum FWHM) in pyroxene refinements did not give structural parameters that were as reasonable for the $C2/c$ pyroxene structure as did step scans using narrower intervals (~ 50% of the minimum FWHM). These step-dependent differences in the refinements presumably result from the complexity of the pyroxene structure (as compared to the simpler compounds used in the above studies), with severe peak-overlap at high diffraction-angles likely being responsible for ill-conditioned refinements of the peak-width parameters, especially U, V and W. Indeed, the derivation of these parameters was quite difficult for some refinements. The maximum step-width that still gave realistic atomic parameters (based on comparison with single-crystal pyroxene structures) was 0.12°2θ, with step counting times of 2 s. Step counting times of 2 s gave maximum step intensities of 2300–4600 counts (Table 2), within a range where counting statistics dominate other sources of uncertainty; values of the standard deviations are correctly estimated in this case. However, as the step width was less than optimum, values of the standard deviations in these refinements are probably slightly underestimated owing to effects of minor serial correlation; this will be shown to be the case for diopside. However, the accuracy of the structural parameters is good.

Details of data collection and structure refinement are given in Table 2, cell dimensions are given in Table 3, and final atomic parameters are presented in Table 4, where they are compared with corresponding data from the single-crystal structural study of diopside (Levien & Prewitt 1981); refined site-occupancies are given in Table 5. The intensity

TABLE 5. REFINED SITE-OCCUPANCIES FOR SYNTHETIC CLINOPYROXENE

		D0	D2	D3	D5	D7
M(1)	Mg	1.00	0.82(1)	0.74(1)	0.52(2)	0.34(2)
	Fe	–	0.18(1)	0.26(1)	0.48(2)	0.66(2)
M(2)	Ca	0.89(2)	1.00	1.00	1.00	1.00
	Mg	0.11(2)	–	–	–	–
	Fe	–	–	–	–	–

data are available from the Depository of Unpublished Data, CISTI, National Research Council of Canada, Ottawa, Ontario K1A 0S2. In general, the various indices of agreement show that the fits between the observed and calculated patterns are quite good, with the whole-pattern index (R_{wp}) varying between 9.7 and 11.4%. The conventional Bragg indices (R_B) evaluate the model fit of the individual peaks, and vary between 3.2 and 3.5%. In these single-phase refinements, there were other minor phases present in amounts too small to be adequately refined as additional phases. Their presence generally contributes far more to the background than to the Bragg peaks of the major phases, and consequently the R_{wp} is slightly higher than one would expect for R_B values of 3–3.5% on pure phases.

The key pieces of information derived from each refinement are the site occupancies. For the Fe-bearing pyroxenes, the occupancy of the $M(2)$ position was refined first as Ca + Fe; this resulted in insignificantly small negative occupancies of $M(2)$ by Fe. As expected, further refinement of $M(2)$ occupancy as Ca + Mg produced insignificantly small positive $M(2)$ occupancies of Mg, and consequently the $M(2)$ occupancy was considered as fixed at 1.0 Ca. This was not the case for diopside, which refined to significant occupancy of $M(2)$ by Mg. Several sets of data were collected on this diopside sample, and the refinements *consistently* showed ~10% substitution of Mg at the $M(2)$ site.

For the $M(1)$ site, the occupancy was refined as Mg + Fe, except for diopside, in which it was fixed at 1.0 Mg, making the crystal-chemically reasonable assumption (borne out by the observed $<M(1)\text{–}O>$ distance) that Ca will not substitute for Mg at $M(1)$.

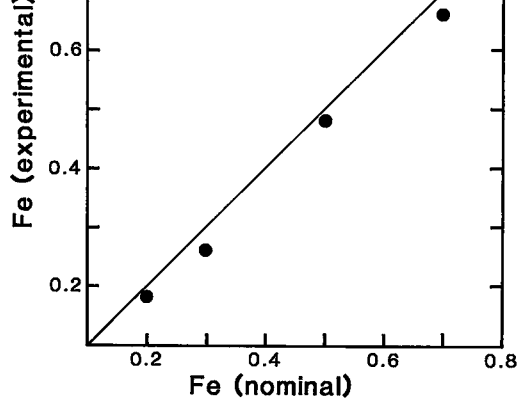

FIG. 2. Comparison of refined synthetic clinopyroxene $M(1)$ site-occupancies with nominal values for 100% synthesis of clinopyroxene.

Unconstrained site-occupancy refinement converged to values that do not deviate by more than 2.7 standard deviations from values suggested by the nominal compositions of the run products.

Structure refinement of two phases

A significant feature of the Rietveld method is its intrinsic capability to refine more than one phase simultaneously. This attribute is very important to the characterization of synthesis products, because they commonly are multiphase. In this study, three of the products (D0, D2 and D3, Table 1) comprise more than 98% pyroxene, and each was refined as a single phase; the others (D5, D7, Table 1) contain up to ~8% ferrobustamite, and were refined as two phases. Ferrobustamite has a complex structure; it is triclinic, $P\bar{1}$, with 16 independent atoms in the asymmetric unit. Because ferrobustamite is present in only small amounts, it was not possible to totally refine its structure; however, this constraint is not a problem, as the ferrobustamite structure is well known from previous single-crystal refinements (Rapoport & Burnham 1973), and we are interested in producing accurate refinements of the host pyroxene by allowing for the presence of ferrobustamite. By fixing the ferrobustamite positions and refining only the scale factor and site occupancies, we could greatly improve the corresponding pyroxene refinements; thus for the two-phase samples D5 and D7, the one-phase R_{wp} and clinopyroxene R_B indices were 12.1, 18.0% and 4.32, 6.48%, respectively, compared with the corresponding two-phase R_{wp} and R_B indices of 8.0, 8.8% and 1.78, 2.49%, respectively. The ferrobustamite site-occupancies also give us the ferrobustamite composition, and the scale factors give us a relative measure of the modal amounts of each phase. R_B indices (3.13, 3.57%) for the second-phase refinements of ferrobustamite are surprisingly low, in spite of refinement of only one experimental parameter (scale factor) and ten structure parameters (cell dimensions, M-site occupancies) out of a possible fifty-eight variables.

The clinopyroxene site-occupancy results for the two-phase refinements parallel those of the single-phase refinements. There is insignificant Fe or Mg at $M(2)$, and the $M(2)$ occupancies were set at 1.0 Ca for the final cycles of refinement. The unconstrained $M(1)$ site occupancies agree fairly well with those expected for the nominal compositions. The results for all the clinopyroxenes refined here are shown in Figure 2. There is a slight but systematic deviation between the refined and nominal compositions, which will be discussed in detail in a later section.

For the two-phase refinements, it is probable that the clinopyroxene does deviate from the nominal composition, otherwise there seems no reason for the existence of the second (ferrobustamite) phase. Is this

TABLE 6. INTERATOMIC DISTANCES (Å) AND ANGLES (°) FOR CLINOPYROXENE

	Di[1]	D0	D2	D3	D5	D7
T–O(1)	1.602(3)	1.606(8)	1.610(7)	1.604(8)	1.616(11)	1.596(12)
T–O(2)	1.589(1)	1.594(8)	1.579(7)	1.586(8)	1.593(11)	1.604(12)
T–O(3)*a*	1.669(3)	1.667(10)	1.674(10)	1.662(11)	1.662(17)	1.685(19)
T–O(3)*b*	1.687(3)	1.697(10)	1.681(10)	1.688(11)	1.673(13)	1.676(15)
⟨T–O⟩	1.637(1)	1.641(4)	1.636(4)	1.635(5)	1.636(7)	1.640(7)
$\langle T\text{–}O\rangle_{nbr}$	1.596(2)	1.600(6)	1.594(5)	1.595(6)	1.605(8)	1.600(9)
$\langle T\text{–}O\rangle_{br}$	1.678(2)	1.682(7)	1.678(7)	1.665(8)	1.668(11)	1.681(12)
M(1)–O(1)*c* ×2	2.119(2)	2.139(11)	2.141(9)	2.153(10)	2.146(15)	2.187(17)
M(1)–O(1)*d* ×2	2.060(7)	2.055(8)	2.056(8)	2.082(8)	2.115(13)	2.099(14)
M(1)–O(2)*e* ×2	2.051(2)	2.031(10)	2.071(8)	2.065(10)	2.060(14)	2.059(15)
⟨M(1)–O⟩	2.076(2)	2.075(4)	2.089(4)	2.100(4)	2.107(6)	2.115(5)
M(2)–O(1) ×2	2.363(2)	2.325(10)	2.348(9)	2.333(10)	2.326(16)	2.335(19)
M(2)–O(2)*f* ×2	2.346(8)	2.345(8)	2.345(8)	2.325(8)	2.316(13)	2.344(15)
M(2)–O(3)*g* ×2	2.561(4)	2.580(9)	2.570(8)	2.577(9)	2.590(13)	2.622(14)
M(2)–O(3)*h* ×2	2.721(4)	2.741(10)	2.730(10)	2.742(12)	2.761(20)	2.723(21)
⟨M(2)–O⟩	2.498(3)	2.498(3)	2.498(3)	2.494(4)	2.498(6)	2.506(6)
T*i*–O(3)–T*j*	135.79(5)	136.1(6)	135.6(6)	136.5(7)	137(1)	135(1)
O(3)*b*–O(3)–O(3)*j*	166.37(6)	165.7(7)	166.4(7)	166.2(8)	167(10)	165(1)

a: $x, y, -1+z$; *b*: $x, -y, -\frac{1}{2}+z$; *c*: $x, 1+y, z$; *d*: $x, 1-y, \frac{1}{2}+z$; *e*: $\frac{1}{2}-x, \frac{1}{2}+y, \frac{1}{2}-z$;
f: $\frac{1}{2}-x, \frac{1}{2}-y, 1-z$; *g*: $\frac{1}{2}-x, \frac{1}{2}+y, \frac{3}{2}-z$; *h*: $\frac{1}{2}-x, \frac{1}{2}-y, 1-z$; *i*: $x, y, 1+z$; *j*: $x, -y, \frac{1}{2}+z$.

[1]diopside, single-crystal structure (Levien & Prewitt 1981)

deviation significant? The ferrobustamite is more Fe-rich than the nominal composition of the clinopyroxene. Using the site occupancies and relative scale-factor for ferrobustamite in sample D7, the composition of the coexisting pyroxene can be calculated from the original bulk-composition of the mix. An *M*(1) occupancy of 0.68 Fe results, compared with the refined occupancy of 0.66(2) Fe and the nominal occupancy of 0.70 Fe. Thus the deviation of the refined pyroxene composition from the nominal composition is in line with the occurrence of (and site occupancies obtained for) the coexisting (more Fe-rich) ferrobustamite.

Pyroxene Stereochemistry: Comparison with Single-Crystal Results

The Rietveld-derived interatomic distances and angles (Table 6) and site occupancies (Table 5) of pyroxene were used to evaluate the reliability of the method by comparison with single-crystal structure data for diopside (Levien & Prewitt 1981), hedenbergite (Cameron *et al.* 1973) and $CaCoSi_2O_6$ (Ghose *et al.* 1987).

Diopside

It is worthwhile to examine the diopside separately as we have both Rietveld and single-crystal results on what is ostensibly material of the same composition. Figure 3 shows a half-normal probability analysis of the Rietveld and single-crystal results for the atomic positions. Data sets containing random normal distributions of errors should give a linear plot of unit slope with zero intercept. The plot is not quite linear, suggesting the presence of a slight systematic error in one or both sets of data. In addition, the slope of ~1.6 (as compared to the ideal value of 1.0) indicates that the *pooled* standard deviations are underestimated by a factor of 1.6. The standard deviations for the Rietveld data are approximately an order of magnitude larger than those for the single-crystal data, and thus the Rietveld values totally dominate the values of the pooled standard deviations. As Figure 3 shows that the latter are underestimated, either the Rietveld values are slightly underestimated or the single-crystal values are underestimated by about an order of magnitude. Comparison of different single-crystal refinements

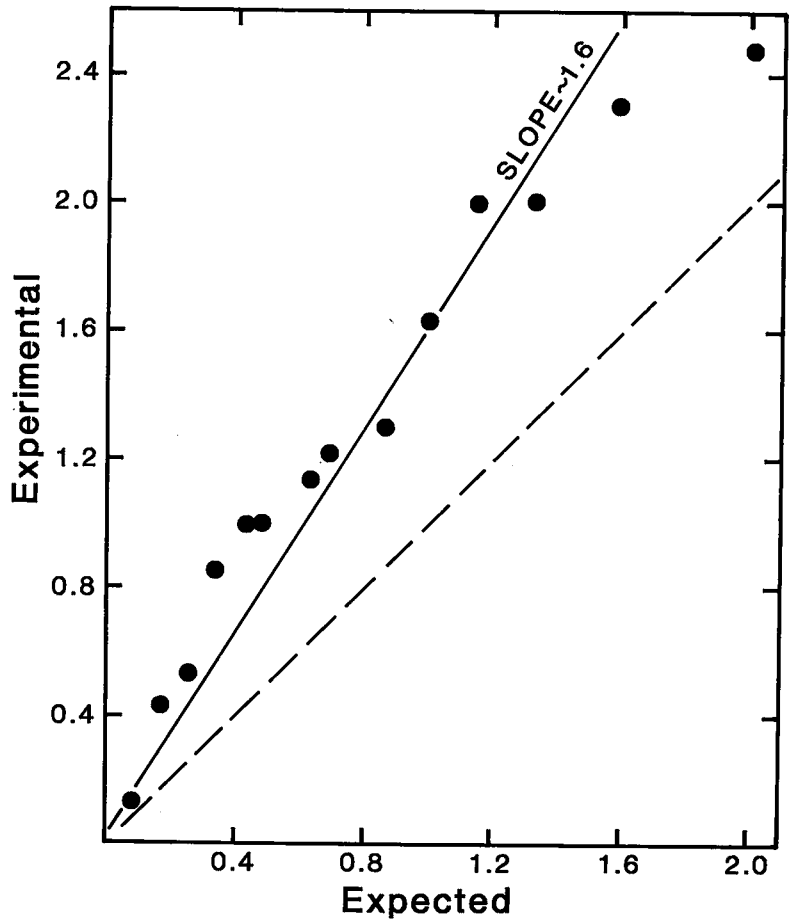

FIG. 3. Half-normal probability analysis of Rietveld and single-crystal positional parameters for diopside.

of diopside (Clark *et al.* 1969, Levien & Prewitt 1981) shows that the single-crystal standard deviations are approximately correct. Consequently the underestimation of the pooled standard deviations must virtually entirely be a result of the underestimation of the Rietveld standard deviations. Of course, this is what we expect, as this is the result of serial correlation, which leads to a systematic underestimation of the assigned standard deviations in Rietveld refinement. As discussed previously, the Durbin–Watson statistic is a measure of this effect (Hill & Flack 1987). The value of 1.39 for the diopside refinement (Table 2) is considerably less than the ideal value of 2.0 ± 0.3, indicating the presence of significant serial correlation that will adversely affect the standard deviations. The Durbin–Watson statistic for diopside is also less than the values obtained for the other pyroxene refinements (Table 2). This is a result of the fact that the individual Bragg diffraction peaks in diopside are markedly wider than the Bragg diffraction peaks in the Fe-bearing pyroxenes.

There is obviously a trade-off here between getting accurate atomic parameters and getting correct standard deviations. If we increase the step interval too much (we examined values up to $0.25°2\theta$), the refined parameters begin to degrade, particularly where there is significant overlap of peaks in the pattern. Conversely, too small an interval gives badly underestimated standard deviations. The step-scan values we used (based on the work of Hill & Madsen 1984) seem a reasonable compromise, but a closer examination of this point on a series of known structures is desirable (and is currently under way).

This kind of analysis gives us a good statistical measure of agreement between the two techniques, but leaves us with no intuitive feel for the agreement between crystal-chemical parameters. Such a comparison is made for selected interatomic distances in

Table 6. The mean polyhedral distances agree extremely well, within one pooled mean standard deviation in each case. If this agreement proves to be generally true, it should be possible to use such mean bond-lengths with pre-existing mean bond-length – site-occupancy curves to derive degree of order and bulk chemical information for those cases in which there is not sufficient difference in scattering power to do so directly from the intensity data. Thus Al/Si order *may* possibly be accessible from (*T*–O) bond lengths for example.

As expected, deviation of individual bond-lengths from the single-crystal values is a little greater than that for the mean polyhedral distances, with maximum differences of 0.038 Å for *M*(2)–O(1) and 0.020 Å for *M*(1)–O(1)*c* and *M*(1)–O(2)*e*. However, in terms of the assigned standard deviations, there is only one significant discrepancy: *M*(2)–O(1), with a difference of 3.8 pooled standard deviations. Even the chain angles *Ti*–O(3)–*Tj* and O(3)*b*–O(3)–O(3)*j* show good agreement. Thus the agreement for diopside stereochemistry is excellent. Of course, we can never achieve results as good as for single-crystal data, because we are collapsing our data into two dimensions, with the consequent loss of information due to overlap. Nevertheless, the method seems capable of accurate results with useful precision.

Intermediate compositions

For the pyroxenes of intermediate composition, we have no analogous crystal-structure results for

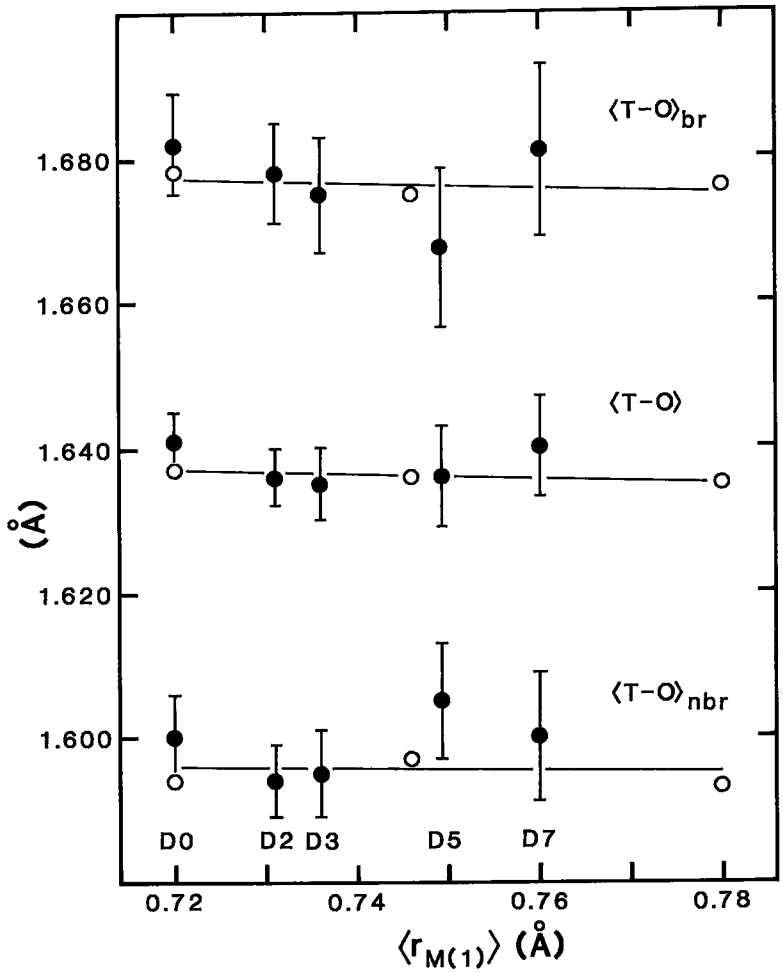

FIG. 4. Variation in $<T\text{-O}>$, $<T\text{-O}>_{br}$ and $<T\text{-O}>_{nbr}$ with mean ionic radius of the constituent cations at the *M*(1) site (solid symbols). Open symbols are single-crystal data for diopside (Levien & Prewitt 1981), $CaCoSi_2O_6$ (Ghose *et al.* 1987) and hedenbergite (Cameron *et al.* 1973).

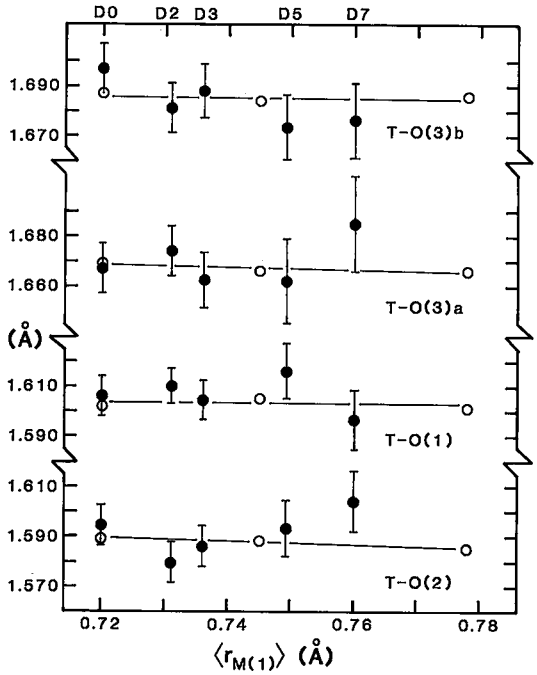

FIG. 5. Variation in individual tetrahedral distances with mean ionic radius of the constituent cations at the $M(1)$ site. Symbols are as in Figure 4.

comparison. However, we can assume that the variations in (at least most) metric properties are linear between those of diopside and hedenbergite.

Tetrahedral chain. There is one unique, tetrahedrally coordinated site in diopside – hedenbergite pyroxenes; this is occupied solely by Si, and the mean T–O distances should be similar across the join. Figure 4 shows the variation in $<T\text{–O}>$, $<T\text{–O}>_{br}$ and $<T\text{–O}>_{nbr}$ distances with mean ionic radius of the constituent cations at the $M(1)$ site; in addition, single-crystal-derived bond lengths of diopside, $CaCoSi_2O_6$ and hedenbergite are shown. All values are consistent with the single-crystal trends. Variation of individual T–O distances with $M(1)$ occupancy is less regular (Fig. 5), and the variation from structure to structure is larger than for the average distances, but all bond lengths are within one or two standard deviations of the correlations for the single-crystal data. Thus within the precision of these data, there is no systematic variation of the T–O bond lengths as a function of $M(1)$ site occupancy, the scatter being a result of the inherently lower resolution of powder technique of structure refinement.

Octahedral strip. Ca-rich pyroxenes on the diopside – hedenbergite join have two unique sites in this structural unit, the [6]-coordinated $M(1)$ site with octahedral coordination, and the larger [8]-coordinated $M(2)$ site. In ordered $C2/c$ pyroxenes,

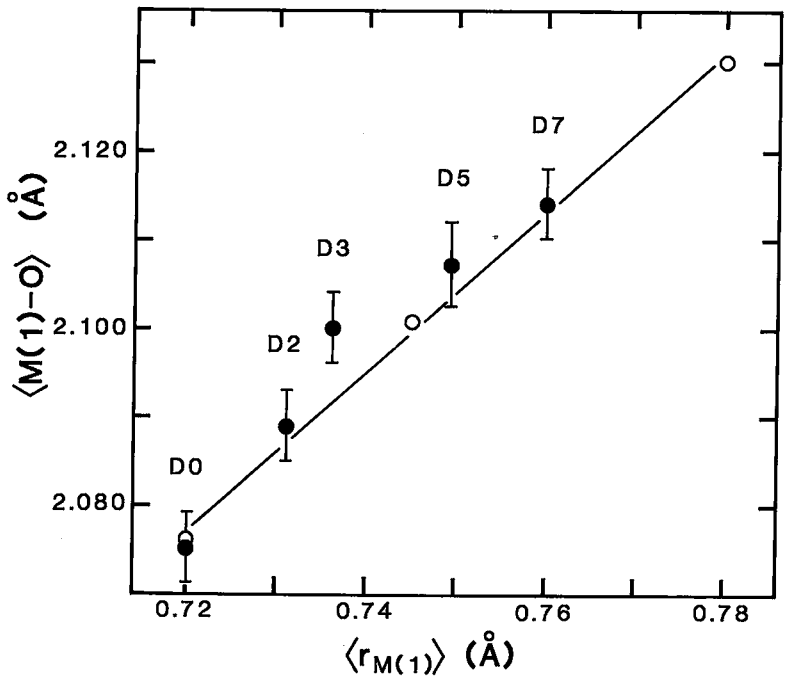

FIG. 6. Variation in $<M(1)\text{–O}>$ with mean ionic radius of the constituent cations at the $M(1)$ site. Symbols are as in Figure 4.

the $M(2)$ site is occupied by Ca, with Fe and Mg ordered at the $M(1)$ site. Many groups of isomorphous structures show a nearly linear relationship between the mean bond-lengths of cation polyhedra and the mean ionic radius of the constituent cations at those sites. Figure 6 shows the variation in $<M(1)\text{–}O>$ as a function of the mean ionic radius for the constituent $M(1)$ cations. Samples D3 and D5 are displaced (one to two standard deviations) to slightly larger $<M(1)\text{–}O>$ distances from the trend line for the single-crystal structures and the other samples from this study. The small displacements shown in Figure 6 are likely due to discrepancies in one or more of the individual $M(1)$–O bond lengths, rather than incorrect site-occupancies; on this plot, any reasonable changes in site occupancies have little effect on the magnitude of the mean ionic radius. Furthermore, our work on amphiboles (Raudsepp *et al.* 1987a, b) has shown that even though quite inaccurate bond-lengths may sometimes be obtained from some Rietveld refinements (owing to pseudosymmetry), the site occupancies are generally accurate and not as sensitive to minor discrepancies in the refinements (provided they are unrelated to the pseudosymmetry aspects of the structure). Figure 7 shows the variation in the individual $M(1)$–O bond lengths with the mean ionic radius of the constituent $M(1)$ cations. All distances are within two standard deviations of the single-crystal trends, but there do seem to be some systematic differences. For $M(1)$–O(1)*d* and $M(1)$–O(2)*e*, the powder values seem to scatter randomly about the single-crystal correlations. However, for the $M(2)$–O(1)*c* bond, although the differences between the powder and single-crystal data do not exceed two standard deviations, the Rietveld-derived distances are systematically longer.

In ordered $C2/c$ calcic pyroxenes, the $M(2)$ site is solely occupied by Ca. However, in spite of identical $M(2)$ occupancy, $<M(2)\text{–}O>$ increases with increasing size of the $M(1)$ cation (Cameron & Papike 1981). Figure 8 shows the variation in $<M(2)\text{–}O>$ and individual $M(2)$–O distances with the mean ionic radius of the constituent $M(1)$ cations. The Rietveld-derived $<M(2)\text{–}O>$ distances follow the single-crystal trend fairly closely, and show an increase as expected. The individual $M(2)$–O distances vary more irregularly. For $M(2)$–O(2)*f*, $M(2)$–O(3)*g* and $M(2)$–O(3)*h*, the Rietveld values are consistent with the single-crystal trends, but for $M(2)$–O(1), although the deviations from single-crystal values are all within about two standard deviations, the Rietveld-derived distances are systematically shorter than those from the single-crystal refinements. Note that there seems to be a correlation between the maximum systematic deviations from the single-crystal trends for the $M(1)$–O and $M(2)$–O bond lengths: $M(1)$–O(1)*c* is systematically longer, and $M(2)$–O(1) is systematically shorter. Examination of the local

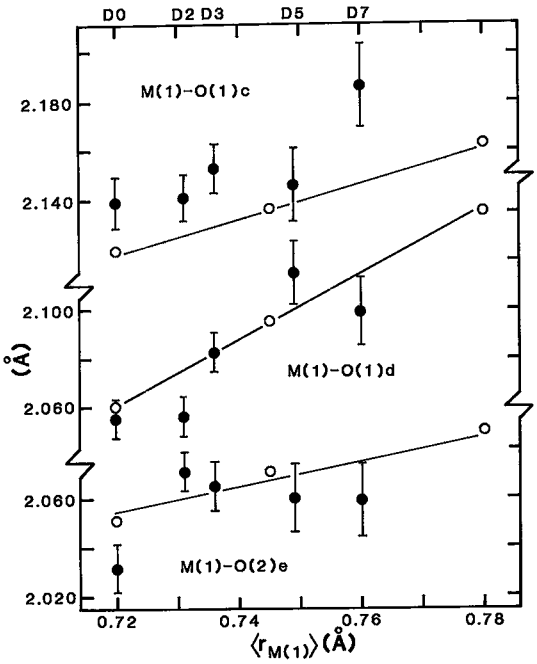

FIG. 7. Variation in individual $M(1)$–O distances with mean ionic radius of the constituent cations at the $M(1)$ site. Symbols are as in Figure 4.

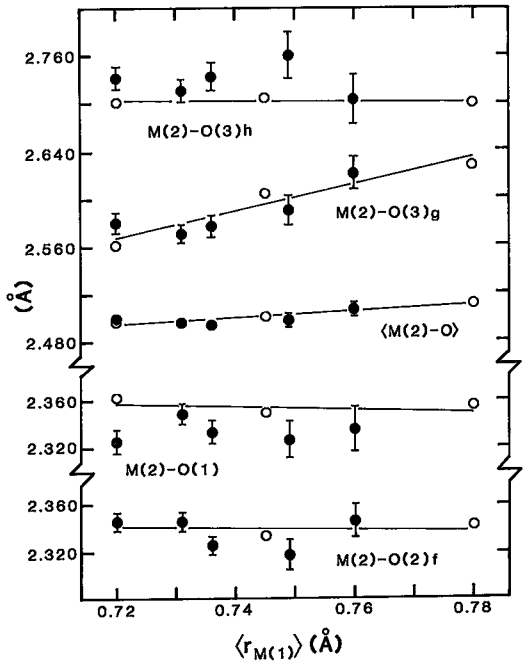

FIG. 8. Variation in $<M(2)\text{–}O>$ and individual $M(2)$–O distances with mean ionic radius of the constituent cations at the $M(1)$ site. Symbols are as in Figure 4.

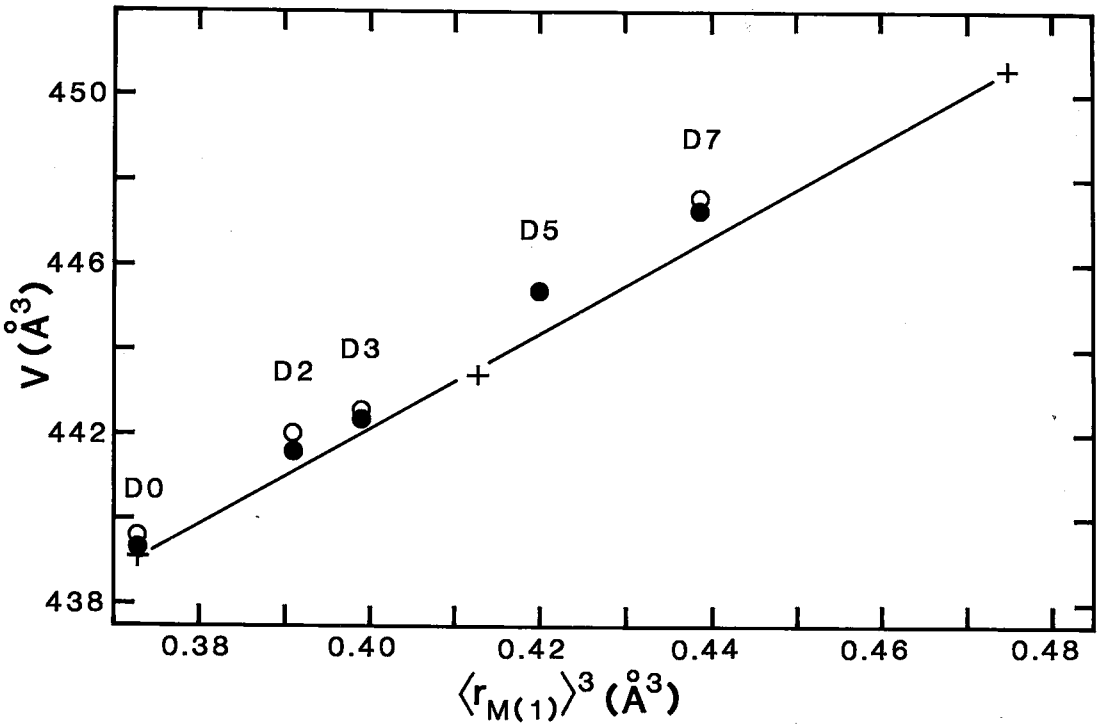

FIG. 9. Variation in cell volume with mean ionic radius cubed of the constituent cations at the $M(1)$ site (solid circles). Open circles represent data from Turnock *et al.* (1973); crosses are data from the single-crystal studies analogous to Figures 4-8.

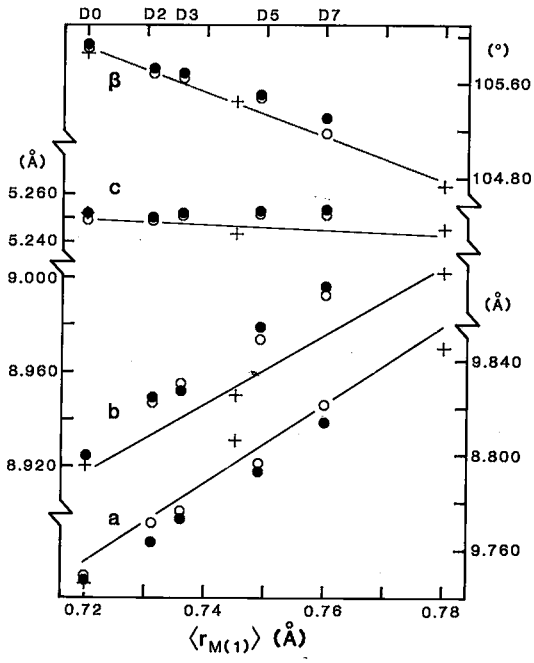

FIG. 10. Variation in cell parameters a, b, c and β with mean ionic radius of the constituent cations at the $M(1)$ site. Symbols are as in Figure 9.

stereochemistry about O(1) suggests that the observed systematic variations result from underestimation of the y coordinate of O(1). Comparison of this parameter with a linear interpolation of y O(1) for diopside and hedenbergite indicates that this is indeed the case. This deviation is reproducible, and several different refinements showed y O(1) to be systematically larger than the corresponding interpolated values; we have no explanation for this, but note that it does not lead to major disparities in the structural parameters of interest.

Cell dimensions. Cell dimensions are sensitive indicators of compositional variation in an isostructural series. Prewitt & Shannon (1969) have shown that the cell volume is a linear function of the cube of the octahedral radius of the variable cation; although Hawthorne (1978) has shown that this relationship is intrinsically nonlinear, the variation in cation radius in this pyroxene series is sufficiently small that a linear model is adequate. As two octahedral cations are involved here, the plot involves the cubed weighted average of the Mg and Fe radii calculated from site occupancies (Fig. 9). Also shown are cell volumes compiled by Turnock *et al.* (1973) for the same samples and from other pyroxene syntheses; the correspondence between the former and the latter is excellent. Both these powder-data sets are slightly displaced to larger volumes with respect to the single-

crystal results, but the trend is close to being linear.

Figure 10 shows the variation in the *a*, *b*, *c* and β cell dimensions with the mean radius of the constituent *M*(1) cations. Again the trends are close to being linear, and the correspondence between the Rietveld-derived parameters and those both measured and compiled independently by Turnock *et al.* (1973) is excellent. However, there are some discrepancies between our data and the single-crystal values. Parameters *a*, *c* and β show linear trends close to those of the single-crystal structures, but *b* systematically diverges with increasing Fe content, being about 0.25% larger than the extrapolated single-crystal value at Fe/(Fe+Mg) = 0.70.

Cation order. Characterization of order among octahedral cations in the diopside – hedenbergite series is facilitated by the large difference in scattering power between Mg and Fe^{2+}. *M*(1) site occupancies were refined without compositional constraints. *M*(1) site occupancies (Table 5) show that the pyroxenes from run products D2, D5 and D7 are essentially nominal in composition (within one to two standard deviations), but D3 is somewhat more Mg-rich. It also deviates most on a plot of $<M(1)\text{–}O>$ *versus* mean *M*(1) cation radius (Fig. 6); however, its position here would not be improved significantly by assuming the nominal composition.

Initially, the *M*(2) occupancy was fixed at 1.00 Ca, and the *M*(1) site occupancies were refined. In subsequent refinements, the occupancy of the *M*(2) site also was allowed to vary. The *M*(2) site occupancies of all the Fe-bearing pyroxenes refined to within one standard deviation of 1.00 Ca; the *M*(2) occupancy of diopside, however, refined to 0.89(2) Ca + 0.11(2) Mg. In the light of previous work on the synthesis and characterization of tremolite, this is a significant result. Jenkins (1987) showed that tremolite synthesized from many starting materials (oxide mixes, gels, crystalline phases) is enriched by ~10% in Mg (Ca depleted). If this is the case for diopside, there should be significant additional Ca-rich phases present; the only observed extraneous phase is a trace of cristobalite. We are forced to conclude that this occupancy of *M*(2) by Mg is an artifact of the refinement.

Bulk Composition from Rietveld Refinement

Diffraction is a spatially resolved electron-counting technique, and with sufficient accuracy and precision, is therefore a technique of chemical analysis. As is apparent from the previous discussion, we are determining site-occupancies with quite reasonable precision (even allowing for the problem of its underestimation). We can deal with the site occupancies in two ways: (i) we can constrain them such that their sum must equal the bulk value for the material; (ii) we can refine them unconstrained. If we choose

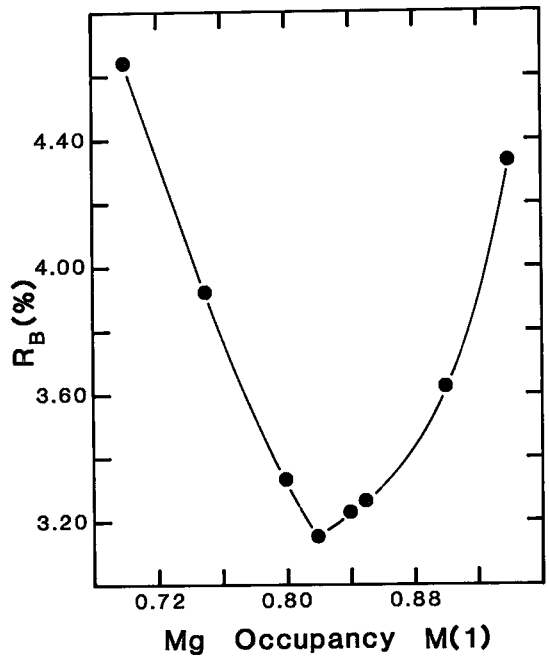

FIG. 11. Variation in R_B index as a function of *M*(1) occupancy for clinopyroxene D2; note the sharp asymmetrical minimum.

to follow method (i), we have *made an assumption* concerning the synthesis process, an assumption that previous work (Hawthorne 1983b and references therein) has shown to be not necessarily true. It is obviously preferable to follow method (ii) and determine the mineral composition, *provided that this can be done accurately*. Although we examine the details of unconstrained site-occupancy refinement elsewhere (Hawthorne *et al.*, unpublished ms.), a brief discussion along these lines is warranted for the current results.

How well-defined is the minimum with regard to the occupancy parameters in an unconstrained least-squares refinement? In principle, this is indicated by the assigned standard deviation(s); however, this criterion ignores the presence of neighboring false minima. We can examine this point by mapping out the value of the residual as a function of the parameter(s) of interest. This we have done for the *M*(1) occupancy of sample D2. The structure of clinopyroxene D2 was refined with the occupancy of *M*(1) fixed at a series of values spanning the nominal composition ±0.12 Mg p.f.u. The results are shown in Figure 11. The minimum seems very well-defined; it is slightly displaced from the nominal composition of 0.80 Mg, and it is apparent that the R_B index is quite sensitive to the occupancy parameter. Similar results for the *M*(2) occupancy

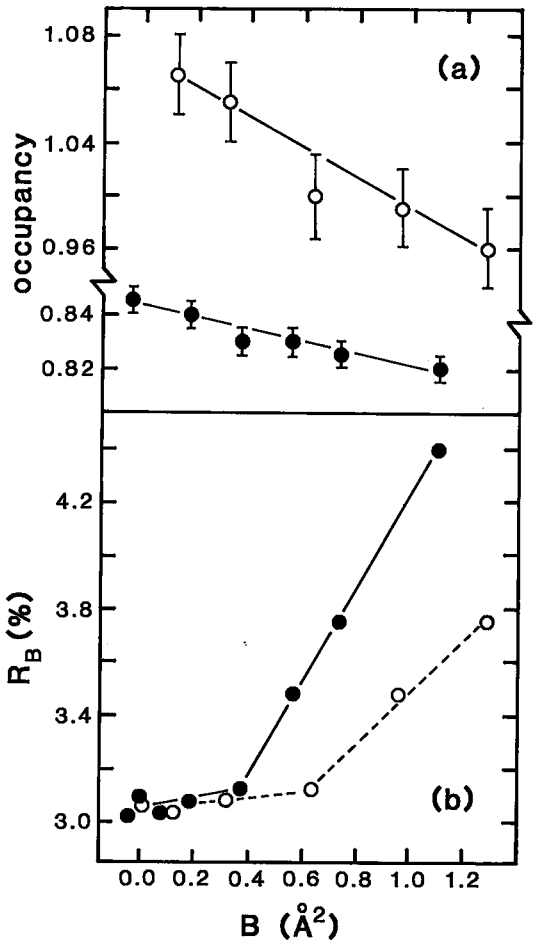

FIG. 12. (a) Variation in $M(1)$ (solid symbols) and $M(2)$ (hollow symbols) occupancy [$M(1) = x\text{Mg} + (1-x)\text{Fe}$; $M(2) = y\text{Ca} + (1-y)\text{Fe}$] as a function of isotropic displacement factor B for clinopyroxene D2; (b) variation in R_B index as a function of $M(1)$ (solid symbols) and $M(2)$ (hollow symbols) isotropic displacement factor for clinopyroxene D2.

show that we can expect quite *precise* results from such occupancy refinements.

What about accuracy? We have discussed this aspect somewhat with regard to diopside, but need to focus a little more specifically on site occupancies. In least-squares refinement, it is well known that there is significant interaction among occupancy parameters, displacement parameters, and the scale factor (Hawthorne 1983a). If there is $\sin\theta/\lambda$-dependent systematic error in the intensity data, these highly correlated parameters can interact with the systematic error to produce inaccurate results. With improvement in techniques of absorption correction, these problems have been largely overcome for single-crystal intensity data. However, the effects of absorption are a possible source of inaccuracy in Rietveld structure refinement, particularly as this technique has inherently less resolution. Consequently, we have taken a more conservative approach to the refinement procedure. We set the isotropic displacement factors for all atoms equal to the values derived from the single-crystal refinement of the structure. Obviously if these values are not appropriate, the refined site-occupancies (and hence the bulk composition) will not be accurate.

We examined the possible effect of using inappropriate displacement factors by doing a series of refinements with the $M(1)$ and $M(2)$ displacement-factors fixed at arbitary values, but refining all other parameters except the displacement factors for silicon and oxygen, which were still fixed at the corresponding single-crystal values. The results for sample D2 are shown in Figure 12a. As expected, there is an inverse correlation between isotropic displacement factor and site occupancy [expressed as $M(1)$: $x\text{Mg} + (1-x)\text{Fe}$; $M(2)$: $y\text{Ca} + (1-y)\text{Fe}$]. Thus it is obviously important to choose appropriate values for the isotropic displacement factors. Comparing the slopes of these curves to the values of the standard deviations on the site occupancies gives an indication of the sensitivity of this relationship. In each case, ± 1 standard deviation in the site occupancy corresponds to ± 0.25 Å^2 in the isotropic displacement factors; this is quite a significant difference in the values of the isotropic displacement factors, suggesting that significant differences in site occupancies will only be caused by use of (what should seem to be) unrealistic displacement factors.

We also examined the behavior of the R-index during this procedure; it is shown in Figure 12b as a function of the isotropic displacement parameters. For small values of B (including the values used from the single-crystal refinement of the diopside structure), the R_B index is fairly insensitive to the isotropic displacement factor; as B becomes larger, R_B climbs relatively rapidly. Comparison of Figures 12a and 12b indicates that the situation is fairly well constrained. Any significant changes (of the order of ± 0.25 Å^2) to the chosen values of the isotropic displacement factors will lead to less satisfactory results. Increase in the B values by this amount will significantly raise the R_B index. Decrease by this amount will not significantly raise or lower R_B, but will give us a less realistic model (*i.e.*, displacement parameters that we *know* are too small). Thus in the present circumstances at least, the method chosen for the site-occupancy refinements seems satisfactory.

Of course, the optimum method would be to refine both the occupancies and the isotropic displacement factors. When this was done for the D2 sample, the results were as follows: $R_B = 3.03\%$, $M(1) = 0.85(1)$

Mg + 0.15(1) Fe, $B = -0.04$ Å^2; $M(2) = 1.01(3)$ Ca + –0.01(3) Fe, $B = 0.75$ Å^2. The values for $M(2)$ seem reasonable, with the occupancy essentially 1.0 Ca and the isotropic displacement factor not significantly different from the single-crystal value. However, B for $M(1)$ refined to a physically unreasonable value, shifting the $M(1)$ site occupancy by approximately three standard deviations. The most important factor in the assessment of the results of any least-squares refinement is the physical validity of the results. We can discount the results of the simultaneous refinement of occupancy and displacement factor on this basis, and prefer our original refinement. This does indicate the presence of some systematic error in the intensity data, an error that is slightly biasing the refined structure. However, the results of this work do suggest that this error is in fact quite small, and that the Rietveld method can be used to derive site occupancies *and* bulk compositions of minerals when the sample composition and constitution are suitable for this technique.

Conclusions

The Rietveld method has been used to refine the crystal structures of synthetic fine-grained clinopyroxenes along the diopside – hedenbergite join. The following points are of particular interest with regard to the characterization of fine-grained synthetic minerals:

(i) For compositions in which there is significant difference in scattering power among different components, site occupancies can be determined with fairly high accuracy and precision (although problems may arise when the structure has pseudosymmetry); thus structural state may be determined.

(ii) Unconstrained site-occupancy refinement can commonly lead to the determination of bulk mineral compositions, subject to the provisos given in (i); this may be of particular interest when synthesis products are very fine grained.

(iii) More than one phase can be refined simultaneously, and modal amounts of the phases can be recovered from the refinement, together with the degrees of cation order and bulk compositions; how well this can be done depends on the complexity and number of the phases involved, together with the degree of overlap in the powder-diffraction pattern.

(iv) As well as compositional information and very precise cell parameters, we also recover crystal-structure information. Of course, these data are not as precise as corresponding single-crystal information, but for the first time we have been able to retrieve such data from fine-grained powders; lower precision is not an issue when this is the only method of deriving such data.

The Rietveld method is a very powerful way to examine fine-grained single- and multi-phase products of mineral syntheses; it is capable of providing information on structural state (cation order), bulk composition, modal composition and crystal structure. Data collection is rapid, there is good public-domain software for the refinement process, and the necessary equipment (a powder diffractometer) is widely available. It should become a standard technique of product characterization in experimental mineralogy and petrology in the future.

Acknowledgements

We thank J.J. Papike, an anonymous reviewer and R.F. Martin for constructive criticism that substantially improved the manuscript. Financial assistance was provided by the Natural Sciences and Engineering Research Council of Canada in the form of operating grants to F.C. Hawthorne and A.C. Turnock, and an infrastructure grant to F.C. Hawthorne.

References

Baerlocher, C. (1982): *The X-ray Rietveld System*. Institut für Kristallographie und Petrographie, ETH, Zurich.

_____ (1984): The possibilities and the limitations of the powder method in zeolite structure analysis: the refinement of the silica end-member of TPA–ZSM–5. *In* Proc. 6th International Zeolite Conference (Reno, 1983; D. Olson & A. Bisio, eds.). Butterworths, London (823-833).

_____ & Schicker, P. (1987): X-ray Rietveld structure refinement of monoclinic ZSM–5. *Acta Crystallogr.* **A43**, *Suppl.* C-233.

Caglioti, G., Paoletti, A. & Ricci, F.P. (1958): Choice of collimators for a crystal spectrometer for neutron diffraction. *Nucl. Instrum.* **3**, 223-228.

Cameron, M. & Papike, J.J. (1981): Structural and chemical variations in pyroxenes. *Am. Mineral.* **66**, 1-50.

_____, Sueno, S., Prewitt, C.T. & Papike, J.J. (1973): High-temperature crystal chemistry of acmite, diopside, hedenbergite, jadeite, spodumene, and ureyite. *Am. Mineral.* **58**, 594-618.

Clark, J.R., Appleman, D.E. & Papike, J.J. (1969): Crystal-chemical characterization of clinopyroxenes based on eight new structure refinements. *Mineral. Soc. Am., Spec. Pap.* **2**, 31-50.

Durbin, J. & Watson, G.S. (1950): Testing for serial correlation in least squares regression. I. *Biometrika* **37**, 409-428.

_____ & _____ (1951): Testing for serial correlation in least squares regression. II. *Biometrika* **38**, 159-178.

_____ & _____ (1971): Testing for serial correlation in least squares regression. III. *Biometrika* **58**, 1-19.

ERCIT, T.S., HAWTHORNE, F.C. & ČERNÝ, P. (1985): The crystal structure of synthetic natrotantite. *Bull. Minéral.* **108**, 541-549.

GHOSE, S., WAN CH'ENG & OKAMURA, F.P. (1987): Crystal structures of $CaNiSi_2O_6$ and $CaCoSi_2O_6$ and some crystal-chemical relations in $C2/c$ clinopyroxenes. *Am. Mineral.* **72**, 375-381.

HAWTHORNE, F.C. (1978): The relationship between cell volume, mean bond length and effective ionic radius. *Acta Crystallogr.* **A34**, 139-140.

_____ (1983a): Quantitative characterization of site-occupancies in minerals. *Am. Mineral.* **68**, 287-306.

_____ (1983b): Characterization of the average structure of natural and synthetic amphiboles. *Per. Mineral. (Roma)* **52**, 543-581.

_____, ed. (1988): Spectroscopic Methods in Mineralogy and Geology. *Rev. Mineral.* **18.**

_____, RAUDSEPP, M., WILLIAMS, B.L. & HARTMAN, J.S. (1984): Characterization of cation ordering in synthetic amphiboles by Rietveld structure refinement and ^{27}Al and ^{29}Si MAS NMR spectroscopy. *Geol. Assoc. Can. - Mineral. Assoc. Can., Program Abstr.* **9**, 72.

HILL, R.J. & FLACK, H.D. (1987): The use of the Durbin-Watson *d*-statistic in Rietveld analysis. *J. Appl. Crystallogr.* **20**, 356-361.

_____ & HOWARD, C.J. (1986): *A Computer Program for Rietveld Analysis of Fixed-Wavelength X-ray and Neutron Diffraction Patterns.* Australian Atomic Energy Commission (now ANSTO), Lucas Heights Research Laboratories, Menai, New South Wales, Australia, *Rep.* **M112.**

_____ & MADSEN, I.C. (1984): The effect of profile step counting time on the determination of crystal structure parameters by X-ray Rietveld analysis. *J. Appl. Crystallogr.* **17**, 297-306.

_____ & _____ (1986): The effect of profile step width on the determination of crystal structure parameters and estimated standard deviations by X-ray Rietveld analysis. *J. Appl. Crystallogr.* **19**, 10-18.

HUEBNER, J.S. & TURNOCK, A.C. (1980): The melting relations at 1 bar of pyroxenes composed largely of Ca-, Mg-, and Fe-bearing components. *Am. Mineral.* **65**, 225-271.

JENKINS, D.M. (1987): Synthesis and characterization of tremolite in the system H_2O-CaO-MgO-SiO_2. *Am. Mineral.* **72**, 707-715.

KHATTAK, C.P. & COX, D.E. (1977): Profile analysis of X-ray powder diffractometer data: structural refinement of $La_{0.75}Sr_{0.25}CrO_3$. *J. Appl. Crystallogr.* **10**, 405-411.

LARSON, A.C. & VON DREELE, R.B. (1988): *Generalized Structure Analysis System.* Los Alamos National Laboratory, Los Alamos, New Mexico, **LAUR 86-748.**

LEVIEN, L. & PREWITT, C.T. (1981): High-pressure structural study of diopside. *Am. Mineral.* **66**, 315-323.

PREWITT, C.T. & SHANNON, R.D. (1969): Use of radii as an aid to understanding the crystal chemistry of high pressure phases. *Trans. Am. Crystallogr. Assoc.* **5**, 51-60.

RAPOPORT, P.A. & BURNHAM, C.W. (1973): Ferrobustamite: the crystal structures of two Ca,Fe bustamite-type pyroxenoids. *Z. Kristallogr.* **138**, 419-438.

RAUDSEPP, M., HAWTHORNE, F.C. & TURNOCK, A.C. (1984): Derivation of site-occupancies in synthetic pyroxenes and amphiboles by Rietveld structure refinement. *Geol. Soc. Am., Abstr. Programs* **16**, 630.

_____, TURNOCK, A.C. & HAWTHORNE, F.C. (1982): Synthesis and characterization of $^{vi}R^{3+}$ analogues of pargasite and eckermannite. *Geol. Assoc. Can. - Mineral. Assoc. Can., Program Abstr.* **7**, 75.

_____, _____ & _____ (1987a): Characterization of cation ordering in synthetic scandium-fluor-eckermannite, indium-fluor-eckermannite, and scandium-fluor-nyböite by Rietveld structure refinement. *Am. Mineral.* **72**, 959-964.

_____, _____, _____, SHERRIFF, B.L. & HARTMAN, J.S. (1987b): Characterization of synthetic pargasitic amphiboles ($NaCa_2Mg_4M^{3+}Si_6Al_2O_{22}(OH,F)_2$; M^{3+} = Al,Cr,Ga,Sc,In) by infrared spectroscopy, Rietveld structure refinement and ^{27}Al, ^{29}Si and ^{19}F MAS NMR spectroscopy. *Am. Mineral.* **72**, 580-593.

RIETVELD, H.M. (1967): Line profiles of neutron powder-diffraction peaks for structure refinement. *Acta Crystallogr.* **22**, 151-152.

_____ (1969): A profile refinement method for nuclear and magnetic structures. *J. Appl. Crystallogr.* **2**, 65-71.

SPEAR, F.S. (1981): An experimental study of hornblende stability and compositional variability in amphibolite. *Am. J. Sci.* **281**, 697-734.

TURNOCK, A.C. (1962): Preliminary results on melting relations of synthetic clinopyroxenes on the diopside – hedenbergite join. *Carnegie Inst. Wash. Yearbook* **61**, 82.

_____ (1970): Phase relations of synthetic Mg–Fe–Ca pyroxenes. *Am. Mineral.* **55**, 314.

_____, LINDSLEY, D.H. & GROVER, J.E. (1973): Synthesis and unit cell parameters of Ca–Mg–Fe pyroxenes. *Am. Mineral.* **58**, 50-59.

WHITE, E.W. (1964): Microprobe technique for the analysis of multiphase microcrystalline powders. *Am. Mineral.* **49**, 196-197.

WILES, D.B. & YOUNG, R.A. (1981): A new computer program for Rietveld analysis of X-ray powder diffraction patterns. *J. Appl. Crystallogr.* **14**, 149-151.

WILSON, A.J.C. (1963): *Mathematical Theory of X-ray Diffraction.* Centrex, Eindhoven.

YOUNG, R.A. (1980): Structural analysis from X-ray powder diffraction patterns with the Rietveld method. *Symp. Accuracy in Powder Diffraction.* National Bureau of Standards, Gaithersburg, Maryland, 143-163.

_____, MACKIE, P.E. & VON DREELE, R.B. (1977): Application of the pattern-fitting structure refinement method to X-ray powder diffractometer patterns. *J. Appl. Crystallogr.* **10**, 262-269.

Received September 14, 1989, revised manuscript accepted December 4, 1989.